Progress In Electromagnetics Research, PIER 94, 153–173, 2009

THE ORIGIN OF ELECTROMAGNETIC RESONANCE IN THREE-DIMENSIONAL PHOTONIC FRACTALS

U. Sangawa

Advanced Technology Research Laboratories
Panasonic Corporation
3-4 Hikaridai, Seika-cho, Soraku-gun, Kyoto 619-0237, Japan

Abstract—After a report on strange electromagnetic resonances emerging in an isotropic paraelectric Menger sponge (MS) now known as a photonic fractal, vigorous studies began to reveal their properties. However, the mechanics of how the resonances occur is still unknown. This report focuses on the findings that the resonances can be perturbation-theoretically identified as those originally occurring in an isolated dielectric cube, and that they arise within band gaps and uncouple with Bloch modes for a certain multiperiodic lattice. This interpretation is justified by the fact that the MS can be considered as a cube embedded in the lattice rather than the outcome of conventional recursive fractal structuring operations. An experimental formula for resonance conditions already reported can be derived from this interpretation.

1. INTRODUCTION

Since it has been reported in [2] that strange electromagnetic resonances are experimentally observed in an isolated paraelectric object now called a photonic fractal (PF) [8], (a lump of isotropic paraelectric shaped Menger sponge (MS) [1], which is a triadic Cantor-type three-dimensional fractal structure as shown in Figure 1), vigorous studies continue to be carried out, both experimental [3, 5] and theoretical [4, 7, 9]. As a result, basic electromagnetic scattering and resonant properties of the PF were gradually revealed to some extent. However, the fundamentals, such as the mechanics for how the resonance occurs, are still unfamiliar. For example, no physical model explains the already-reported empirical resonance condition [5] for a

Corresponding author: U. Sangawa (sangawa.ushio@jp.panasonic.com).

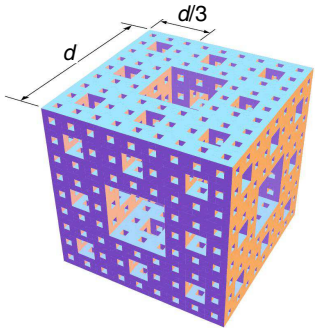

Figure 1. 3-D view of a Stage-3 Menger sponge (MS) with side length d. The Stage-number representing fractal levels of an MS is defined in Section 2.

fundamental mode supported by a PF with side length d and average permittivity $\bar{\varepsilon}_r$ represented in terms of the free space wavelength λ_0,

$$d = \frac{3}{2}\frac{\lambda_0}{\sqrt{\bar{\varepsilon}_r}}, \tag{1}$$

despite its simple expression.

Investigations of the frequency dependencies of transmission properties for a multilayered filter with a Cantor-bar type layer structure (see Figs. 3 and 4 in Reference [10]) corresponding to a one-dimensional rendering of the PF revealed that the resonance condition (1) holds approximately not only for resonant modes in the three-dimensional structure, but also for those in the one-dimensional structure, if one regards d and $\lambda_0/\sqrt{\bar{\varepsilon}_r}$ as the total filter thickness and incident wavelength, respectively. From this finding, it could be conjectured that the same physics governs the resonant modes for both. Moreover, it is crucial that the filter does have a band structure in the transmission spectrum which is typical of periodic potentials, and that resonance peaks always appear in band gaps, although no obvious periodic structure can be recognized in the filter. In addition, (1) suggests that the Cantor-bar type fractal structure must choose the third harmonic among the resonant modes generated by a single film with thickness d and average permittivity $\bar{\varepsilon}_r$. From these intuitions, the generating mechanism of the resonant modes for a PF (hereinafter called those localized modes, following Reference [2])

could be conjectured as follows.

Localized mode specified by (1)	$\approx$	A resonant mode corresponding to the third harmonic originally arises in a dielectric cube with side length d and permittivity $\bar{\varepsilon}_r$. This mode selection is caused by the interaction between non-localized modes (namely, Bloch modes) coming from a certain periodic structure and resonant modes supported by the cube, both structures embedded in the PF.

(2)

This report states that the conjecture of (2) concerning the mechanics of how the localized mode occurs in a PF is justified by applying perturbation theory to mode coupling analyses, and that the experimental condition (1) can be derived as an outcome. In Section 2, by introducing a novel construction method for an MS, we determine that a PF certainly contains a periodic structure. Then, the strategy for mode analysis of PF is clarified via the construction method, and is summarized in Section 3. In Section 4, following the strategy, mode analysis for the periodic and cubic potentials is performed individually, and then the mode couplings between the two are treated using the first perturbation approximation. There, the justification of (2) is given in addition to a derivation of the resonance condition (1). It is also shown in Section 5 that the mechanics can explain some experimental findings hitherto unexplained.

2. NOVEL CONSTRUCTION METHOD FOR AN MS

An MS is a three-dimensional fractal structure possessing evident self-similarity [1] of single scale factor 1/3 between substructures with adjacent fractal levels, as shown in Figure 1. It can be conventionally constructed by recursively operating a set of the following geometrical manipulations on a cube as an initial operand.

(i) Subdivide every initial cube into 27 smaller cubes with the homothetic ratio of 1/3 to the initial cubes.

(ii) Then, remove 7 of the small cubes lying at the center of each side and body of the initial cubes.

The repetition number of the operation is called the Stage-number (MS in Figure 1 has Stage-number 3) and is an important parameter for distinguishing structural differences of MSes. It is almost impossible to extract periodic structures from an MS using this conventional construction method. However, we can devise a novel fractal construction method treating an MS as a unit cell of a multiperiodic

lattice, as depicted in Figure 2. Here, we will denote a potential (concrete definitions will be given below) for a simple cubic lattice as $L^{(1)}(\mathbf{x})$, where $\mathbf{x}$ means a position. For $L^{(1)}(\mathbf{x})$, the lattice constant is (d, d, d), and the primitive cell is a hexapod shape as shown in Figure 3. In addition, the hexapod is composed of three orthogonally crossing rectangular pillars with length d and square cross section of side length $d/3$. We assume that the potential $L^{(1)}(\mathbf{x})$ takes 1 at the outside of the hexapods and 0 inside. If we also label a similar lattice potential with the homothetic ratio $(1/3)^{i-1}$ $(i \geq 2)$ to $L^{(1)}(\mathbf{x})$ as $L^{(i)}(\mathbf{x})$, and a cubic potential with side length d and taking 1 inside and 0 outside as $C(\mathbf{x})$, then a potential $M^N(\mathbf{x})$ for an MS with Stage-N taking 1 inside and 0 otherwise can be expressed in terms of above quantities as follows:

$$M^N(\mathbf{x}) = C(\mathbf{x}) \prod_{i=1}^{N} L^{(i)}(\mathbf{x}) = C(\mathbf{x}) \prod_{i=1}^{N} L^{(1)}\left(3^{i-1}\mathbf{x}\right). \tag{3}$$

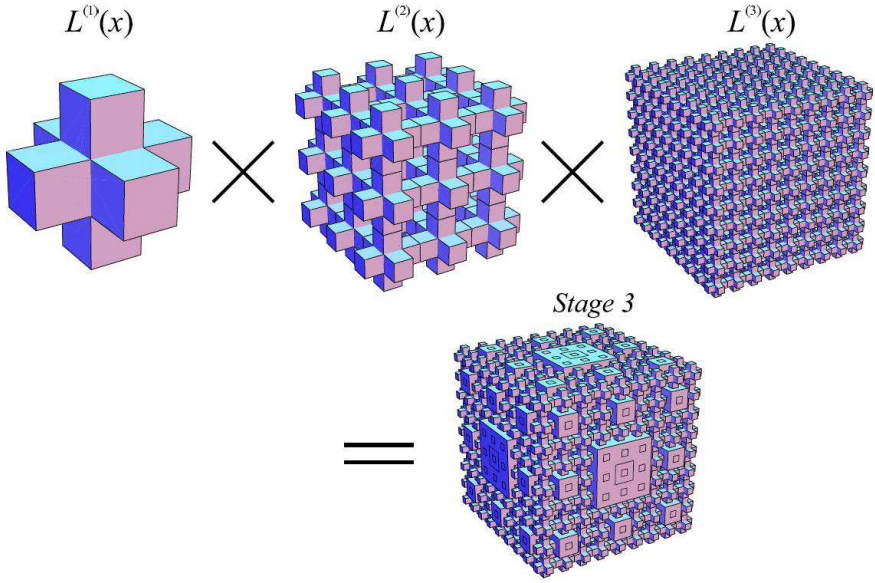

Figure 2. Novel construction method for a Stage-3 MS. The MS can be regarded as a unit cell of a multiperiodic lattice obtained by the product of three similar simple cubic lattices having hexapods at every site. Note that the complement of each potential is shown for easy depiction.

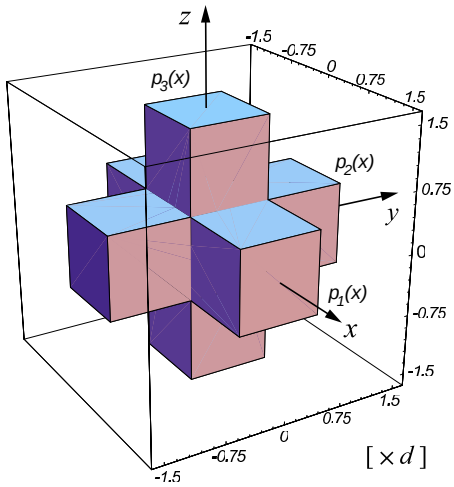

Figure 3. 3-D structure of a hexapod potential: A primitive cell of lattice potential $L^{(1)}(\mathbf{x})$ with lattice constant (d, d, d).

As can be seen in (3) and Figure 2, an MS can be regarded as a primitive cell quarried out from a multiperiodic lattice obtained by the product of ordinal periodic lattices $L^{(i)}(\mathbf{x}) = L^{(1)}(3^{i-1}\mathbf{x})$. Figure 2 schematically shows that an MS with Stage-3 is properly generated according to the novel method (note that complements of $L^{(i)}(\mathbf{x})$ are depicted in the figure for easy visibility). In summary, it was confirmed that a periodic (specifically, multiperiodic) structure certainly occurs in MSes.

3. STRATEGY FOR MODE ANALYSIS OF A PF

In Section 2, it was stated that MSes do contain cubic and (multi-) periodic potentials. As shown in subsequent sections, the isolate cubic potential generates a set of discrete resonant modes in which the electromagnetic energy concentrates into a small spatial area, and the periodic potential supports Bloch modes spreading throughout the space and showing band structures in the dispersion characteristics. The two modes must generally couple with each other within the MS unless there are exceptional conditions, because they are not orthogonal modes. Also, it can be hypothesized that the resonant mode cannot localize, and disappears from MS spectra if coupling or degeneracy occur between the two modes, because part of the localizing energy of the resonant mode is distributed to Bloch modes and carried away

into free space. From this hypothesis, localized modes of the MS can be regarded as originating from resonant modes supported by a cubic paraelectric, and never couple and degenerate to Bloch modes generated by a multiperiodic lattice. Considering conjecture (2), conditions that mode coupling and degeneracy never happen can be interpreted that the two modes are to be orthogonal and resonant modes must appear within band gaps of Bloch modes.

As mode coupling can be suitably dealt with by applying perturbation theory, we will first identify the resonant modes and Bloch modes individually for the zeroth order approximation, and then calculate the coupling among them by treating the former as the first-order perturbation correction to the latter. If we find modes fulfilling the above-mentioned conditions, we will regard them as the origin of localized modes for the MS. In contrast to this treatment, another calculation can be performed by regarding Bloch modes as a perturbation to the resonant modes; this will also be carried out to derive explicit resonant conditions including (1). Mode analysis will be concretely carried forward in subsequent sections using this strategy.

4. THE ORIGIN OF LOCALIZED MODES

4.1. Band Structure of Multiperiodic Lattices

4.1.1. Single Periodic Lattices

To begin, we will summarize the behavior of Bloch modes supported by a single periodic lattice potential within the scope of the weak-coupling approximation (i.e., amplitudes for scattered waves can be regarded as the first-order correction to incidents), in order to introduce quantities and concepts frequently used in subsequent discussion. Monotonic magnetic fields $\mathbf{H}(\mathbf{x})$ with angular frequency ω propagating in an isotropic paraelectric medium with permittivity distribution $\varepsilon_r(\mathbf{x})$ are governed by Maxwell's equations with potential $U(\mathbf{x}) = 1/\varepsilon_r(\mathbf{x})$ and solenoidal condition $\operatorname{div}\mathbf{H}(\mathbf{x}) = 0$ as a constraint,

$$\nabla \times \left\{U(\mathbf{x})\nabla \times \mathbf{H}(\mathbf{x})\right\} - W\mathbf{H}(\mathbf{x}) = \mathbf{0}, \tag{4}$$

where $W = \omega^2/c^2$ (c: Speed of light).

If $\varepsilon_r(\mathbf{x})$ has the periodicity of the simple cubic lattice with lattice constant d, general solutions for (4) can be represented as a linear combination of the Bloch modes $\{|\,\mathbf{n}\rangle\} = \{\mathrm{e}^{\mathrm{i}(\mathbf{k}+\mathbf{P_n})\cdot\mathbf{x}}/\sqrt{d^3}\}$ with corresponding vector-valued expansion coefficients $\{\mathbf{H}(\mathbf{n})\}$, namely

$\mathbf{H}(\mathbf{x}) = \sum_{\mathbf{n}} \mathbf{H}(\mathbf{n})|\mathbf{n}\rangle$. Then $\{|\mathbf{n}\rangle\}$ satisfy the following relations:

$$\mathbf{P_n} = \frac{2\pi}{d}\mathbf{n}, \quad (\mathbf{n} = (n_1, n_2, n_3),\ n_i = 0, \pm 1, \pm 2, \ldots) \tag{5a}$$

$$\langle \mathbf{m}|\mathbf{n}\rangle = \frac{1}{d^3}\int_{1\text{ cell}} d^3x\ \mathrm{e}^{-\mathrm{i}(\mathbf{k}+\mathbf{P_m})\cdot\mathbf{x}}\ \mathrm{e}^{\mathrm{i}(\mathbf{k}+\mathbf{P_n})\cdot\mathbf{x}} = \delta_{\mathbf{mn}}. \tag{5b}$$

Note that the solenoidal condition now becomes $(\mathbf{k}+\mathbf{P_n})\cdot\mathbf{H}(\mathbf{n}) = 0$ for every mode. It can be seen from (5b) that the field distributions $\{\mathbf{H}(\mathbf{n})|\,\mathbf{n}\rangle\} \equiv \{|\,\mathbf{n}\,\rangle\!\rangle\}$ form an orthonormal basis if $|\mathbf{H}(\mathbf{n})|^2 = 1$, and any fields can be expanded into a unique linear combination of this set.

The zeroth and first corrections to an eigenvalue W for (4) associated with every mode can be concretely obtained by applying perturbation expansion to (4) in terms of a perturbation $U(\mathbf{x})$. If the eigenvalue is represented as perturbation expansion $W = W^{(0)} + W^{(1)} + \ldots$ ($W^{(i)}$ means the i-th correction term), plane waves with wavenumbers satisfying the Bragg reflection condition (hereinafter abbreviated as the Bragg condition, and the condition is derived as the pole of the first order approximated amplitude $\mathbf{H}(\mathbf{n})$) $(\mathbf{k}+\mathbf{P_n})^2 = \mathbf{k}^2$ (namely, $\mathbf{k} = -1/2\,\mathbf{P_n}$ if $\mathbf{n} \neq \mathbf{0}$) have the following approximate eigenvalues.

$$W^{(0)} = U(\mathbf{0})\,|\mathbf{k}|^2, \quad (\text{where } U(\mathbf{0}) = 1/\bar{\varepsilon}_r) \tag{6a}$$

$$W^{(1)} = \pm|U(\mathbf{m})|\,|\mathbf{k}|^2 \tag{6b}$$

Here, $U(\mathbf{m})$ means a Fourier coefficient for $U(\mathbf{x})$ with respect to $|\mathbf{m}\rangle$, that is, $U(\mathbf{m}) = \langle\mathbf{m}|\,U(\mathbf{x})|\mathbf{0}\rangle = 1/d^3\int d^3x U(\mathbf{x})\,\mathrm{e}^{-\mathrm{i}\,\mathbf{P_m}\cdot\mathbf{x}}$ (the integral is performed over the primitive cell as shown in (5b)), and $\bar{\varepsilon}_r$ is the averaged permittivity and corresponds to the inverse of $U(\mathbf{0}) = \langle\mathbf{0}|\,U(\mathbf{x})|\mathbf{0}\rangle$.

It can be seen from (6b), under the first approximation, that plane waves cannot propagate at frequencies where the Bragg condition is satisfied, because the interference of scattering waves from the potential becomes dominant, and mode splitting of two degenerating Bloch modes arises, although they could propagate in the entire frequency range under the weak limit $|U(\mathbf{m})|/|\,U(\mathbf{0})| \to 0$. Consequently, the dispersion relation $\bar{\varepsilon}_r\,\omega^2 = c^2|\mathbf{k}|^2$ is slightly modified, and band gaps having frequency width $\Delta W = 2|U(\mathbf{m})||\mathbf{k}|^2$ appear. This outcome suddenly leads to the fact that if $U(\mathbf{m}) = 0$, mode couplings never occur, and Bloch modes can propagate freely even though the Bragg condition is satisfied. This finding is crucial for subsequent analysis.

4.1.2. Band Theory for Multiperiodic Lattice (Recursive Treatment)

Based on the previous subsection, band structures for Stage-N multiperiodic lattice $L^N(\mathbf{x}) = \prod_{i=1}^{N} L^{(i)}(\mathbf{x})$ contained in the potential of MS $M^N(\mathbf{x})$ as in (3) are investigated in this section. Using $L^N(\mathbf{x})$, a potential $U_L^N(\mathbf{x})$ corresponding to a multiperiodic lattice composed of an isotropic paraelectric with permittivity ε_r can be represented as follows:

$$U_L^N(\mathbf{x}) = 1 - \varepsilon_f^{-1} L^N(\mathbf{x}), \quad \left(\varepsilon_f^{-1} \equiv 1 - 1/\varepsilon_r\right). \tag{7}$$

As each sublattice composing $L^N(\mathbf{x})$ has a simple cubic structure, its reciprocal lattice space can be always spanned by $\mathbf{P_n}$, which was already investigated. Since the information about band structures is included only in $-\varepsilon_f^{-1} L^N(\mathbf{m}), (\mathbf{m} \neq \mathbf{0})$ because of (7), below we will focus on $L^N(\mathbf{m})$. Concrete calculations of $L^N(\mathbf{m})$ can be easily performed by applying a fractal construction method already reported in [9] rather than the one developed in Section 2, and the quantities can be directly obtained from the following recursion equations.

$$\begin{aligned} L^{N+1}(\mathbf{m}) &= \frac{1}{3^3} L^N(\mathbf{m}/3)\, AF(\mathbf{P_m}) \\ L^0(\mathbf{m}) &= \operatorname{sinc}(1/2\, \mathbf{P_m}\, d) \\ AF(\mathbf{P}) &= 4\left(\sum_{i=1}^{3} \frac{1}{\cos(1/3\, P_i d)} + 2\right) \prod_{i=1}^{3} \cos(1/3\, P_i d) \end{aligned} \tag{8}$$

Here, $\operatorname{sinc} \mathbf{x} \equiv \prod_{i=1}^{3} \sin x_i / x_i$ and $\mathbf{x} = (x_1, x_2, x_3)$.

Figure 4 shows numerical results of $20 \log_{10} |L^N(\mathbf{m})|$ for Stage-numbers 1 to 4 obtained using (8). Every density graph is normalized by $L^N(\mathbf{0})$, and plotted on a plane $\mathbf{m} = (m_1, m_2, 0)$ with brighter colors representing bigger values. It can be seen from the figure that $L^N(\mathbf{m}) = 0$ exactly holds if vector $\mathbf{m}$ has at least one component equal to multiples of 3^N. As the multiperiodic lattice possesses simple cubic symmetry, Figure 4 demonstrates that band gaps, assigned by wavenumbers $\mathbf{k} = -\mathbf{P}_{\mathbf{m}^N}/2$, which are defined from the Bragg condition and have $\mathbf{m}^N = (3^N l, m, n)$, ($l(\neq 0), m,$ and n are integers) or its permuted vectors (there exist 3! different vectors), definitely cannot open. In other words, two Bloch modes proportional to $|\mathbf{0}\rangle \propto \mathrm{e}^{\mathrm{i}\,\mathbf{k}\cdot\mathbf{x}}$ and $|\mathbf{m}^N\rangle \propto \mathrm{e}^{\mathrm{i}(\mathbf{k}+\mathbf{P}_{\mathbf{m}^N})\cdot\mathbf{x}}$ never couple with each other despite the existence of potential $U_L^N(\mathbf{x})$. This is one of striking properties of the multiperiodic lattice, and plays a crucial role to reveal the origin of localized modes in PFs.

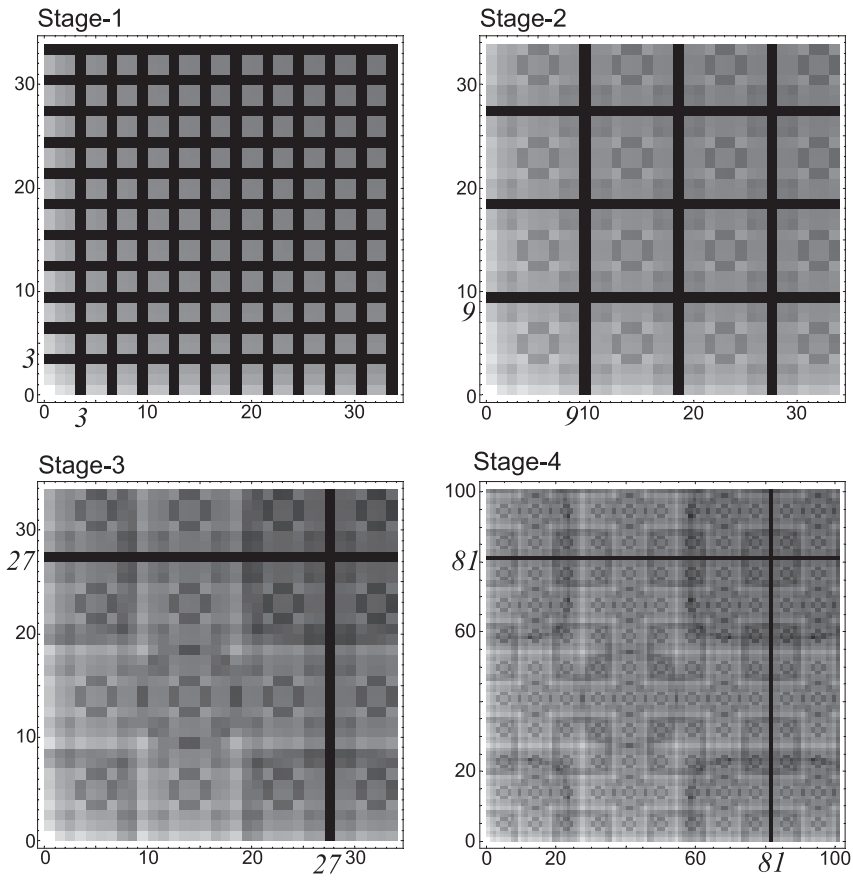

Figure 4. Density plots of Fourier coefficients $L^N(\mathbf{m})$ for multiperiodic lattices of Stage-1 to -4 in a plane with $\mathbf{m} = (m_1, m_2, 0)$. Abscissa and ordinate are assigned by m_1 and m_2, respectively. Brighter colors denote bigger values, and $L^N(\mathbf{m}) = 0$ exactly holds on black lines.

As reported in [9, 10], the self-similarity of fractal structures in real space must be reflected in scattering amplitudes, because the two quantities can be connected through well-defined mathematical manipulations. Therefore, it must be expected that this is also the case for resonant phenomena of PFs, and the self-similarity in the dual space is certainly observed in $L^N(\mathbf{m})$. Figure 5 shows distributions of $L^5(\mathbf{m})$ at various plotting scales. From the upper-left to the lower-right graphs, the plotting area enlarges by about three times. As the figure clearly shows, the Fourier coefficients possess evident self-

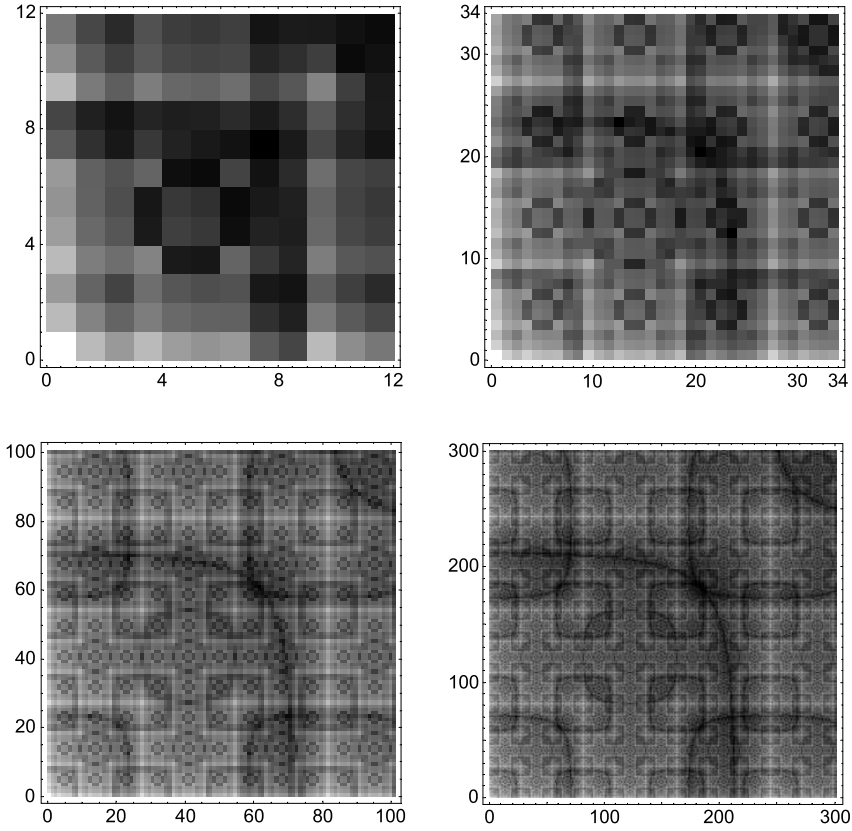

Figure 5. Density plots of Fourier coefficients $L^5(\mathbf{m})$ for Stage-5 multiperiodic lattice. Graph formats are set to the same as Figure 4. Evident self-similarity with the homothetic ratio of 3 can be observed.

similarity of the homothetic ratio 3, which equals the inverse of that in real space. This outcome is thought to be the consequence of the reciprocal property of the Fourier transformation, and the whole self-similar property of PFs must be governed mainly by the properties of multiperiodic lattices only.

4.1.3. Band Theory for a Multiperiodic Lattice (Convolution)

In this section, $L^N(\mathbf{m})$ will be derived again using a different approach from that in the previous subsection because of the need for later perturbation calculations. One can easily represent $L^N(\mathbf{m})$ as an infinite convoluted sum by utilizing generic properties of the Fourier

transformation, because $L^N(\mathbf{x})$ is represented as the simple product of $L^{(i)}(\mathbf{x}), (i = 1, 2, \ldots, N)$, and each $L^{(i)}(\mathbf{x})$ is expressed as the scale transformation of $L^{(1)}(\mathbf{x})$ as in (3).

$$L^N(\mathbf{m}) = \sum_{\left\{\mathbf{n}^{(i)}\right\}} \prod_{i=1}^{N} L^{(1)}\left(\mathbf{n}^{(i)}\right) \delta_{\mathbf{m},\Sigma_{i=1}^{N} 3^{i-1}\mathbf{n}^{(i)}} \tag{9a}$$

$$L^{(1)}(\mathbf{n}) = \delta_{\mathbf{0},\mathbf{n}} - \frac{1}{3^3} \operatorname{sinc}\left(\frac{\pi}{3}\mathbf{n}\right) \left\{ 3 \sum_{i=1}^{3} \frac{\delta_{n_i,0}}{\operatorname{sinc}\left(\frac{\pi}{3}n_i\right)} - 2 \right\} \tag{9b}$$

Here, $\mathbf{n}^{(i)} = (n_1^{(i)}, n_2^{(i)}, n_3^{(i)})$, $(i = 1, 2, \ldots, N)$, and each component takes integral values, namely, $n_j^{(i)} = 0, \pm 1, \pm 2, \ldots$. In addition, the summation for $\{\mathbf{n}^{(i)}\}$ in the first equation runs for all suffixes $n_j^{(i)}$, $(i = 1, \ldots, N,\ j = 1, 2, 3)$. (9a) is complicated, and in order to see what the equation says, we will write down the equation at $N = 2$, for example.

$$L^2(\mathbf{m}) = \sum_{\mathbf{n}^{(1)},\,\mathbf{n}^{(2)}} L^{(1)}\left(\mathbf{n}^{(1)}\right) L^{(1)}\left(\mathbf{n}^{(2)}\right) \delta_{\mathbf{m},\mathbf{n}^{(1)}+3\mathbf{n}^{(2)}}$$

Again, (9b) corresponds to the Fourier coefficient for potential $L^{(1)}(\mathbf{x})$ depicted in Figure 3. Stated previously, the potential is built up by superposing three prisms parallel to each coordinate axis, removing the overlap between them so as to take 1 at the inside of the hexapod, and subtracting the hexapod potential from the uniform background with unity. (9b) reflects this construction procedure. Other constructions can be devised; however, the same expressions must result. $\mathbf{m}^1$ satisfying $L^{(1)}(\mathbf{m}) = 0$ is identified from (9b), and $\mathbf{m}^1 = (3l, m, n)$, $(l(\neq 0), m, n$ are integers) or permuted vectors of $\mathbf{m}^1$ (there exist 3! different vectors) result. In addition, $\mathbf{m}^N$ that meets the condition $L^N(\mathbf{m}) \neq 0$ can be determined from (9a) as follows:

$$\mathbf{m}^N = \mathbf{n}^{(1)} + 3\mathbf{n}^{(2)} + 3^2\mathbf{n}^{(3)} + \ldots + 3^{N-1}\mathbf{n}^{(N)}.$$

These findings lead to the same conclusions as the recursive calculations in the previous section.

4.2. Resonance Conditions for a Paraelectric Cube

In this section, we will investigate resonant modes generated in an isotropic paraelectric cube with side length d and permittivity ε_r, by

applying an approximation calculation method known as the Marcatili-Itoh-Chang method [11, 12], treating electromagnetic fields in the cube as those for a straight rectangular dielectric waveguide with two open ends. According to the method, the cubic resonator generates two sets of modes, the TE-mode TE^x_{pqr} and the TM-mode TM^x_{pqr}, assuming that the waveguide and the dominant polarization for the modes are parallel to the z-axis and x-axis, respectively. (Note that suffixes p, q, and r are integers greater than zero, and absolutely determined from three resonance conditions.) Moreover, one more approximation, regarding evanescent fields around the surface of the cube as negligibly small, is imposed in this report to simplify discussion.

Following the literature with reflecting these assumptions, resonance conditions for both TE- and TM-modes can be expressed in terms of wavenumber $\mathbf{Q_i} = (2\pi/d)\,\mathbf{i}$ defined by a vector $\mathbf{i} = (p, q, r)$ (in the present case, p, q, and r are integers or half-odd integers but they do not take zero simultaneously) as follows:

$$|\mathbf{Q_i}|^2 = \varepsilon_r\, {k_0}^2, \tag{10}$$

where k_0 is the wavenumber in free space and satisfies $\omega = c\,k_0$ (c: Speed of light). To explain the vector $\mathbf{i}$ in more detail, we should note that field distributions in the xy-plane are obtained from single scalar potential $\Phi(x, y)$ [13]. Suffix p takes a half-odd integer when $\Phi(x, y)$ becomes an even function with respect to the x-axis ($\Phi(-x, y) = \Phi(x, y)$), and an integer otherwise (namely, the odd case $\Phi(-x, y) = -\Phi(x, y)$). Similarly, according to the parity of the fields with respect to the z-axis, suffix r also takes integer or half-integer values. However, suffix q takes only integral values.

Then, the resulting set of modes $\{|\mathbf{i})^{\mathrm{m}}_{\mathrm{xz}}\}$ associated with the wavenumber $\mathbf{Q_i}$ are given as follows:

$$|\mathbf{i})^{\mathrm{m}}_{\mathrm{xz}} = C(\mathbf{x}) \sum_{\substack{lmn \\ (l,m,n=0,1)}} \mathbf{H}^{\mathrm{m}}_{\mathrm{xz}}(\mathcal{P}_{lmn}\mathbf{Q_i})\ \mathrm{e}^{\,\mathrm{i}\,\mathcal{P}_{lmn}\mathbf{Q_i}\cdot\mathbf{x}}. \tag{11}$$

In this equation, the superscript "m" distinguishes between TE- and TM-modes, and "x" and "z" denote the parity with respect to the x- and z-axes elucidated above. In addition, $\mathbf{H}^{\mathrm{m}}_{\mathrm{xz}}(\mathbf{h})$ means a vector-valued expansion coefficient for magnetic fields associated with eigenmode $\mathrm{e}^{\,\mathrm{i}\,\mathbf{Q_h}\cdot\mathbf{x}}$, and is a function of wavenumber $\mathbf{h}$ only. $\mathcal{P}_{lmn}$ is a coordinate inversion operator, and acts on any vector $\mathbf{v} = (v_1, v_2, v_3)$ as $\mathcal{P}_{lmn}\mathbf{v} = (\,(-1)^l v_1, (-1)^m v_2, (-1)^n v_3\,)$. (11) simply says that the resonant modes can be regarded as standing waves generated by 8 plane waves with wavenumbers $2\pi/d\,(\pm p, \pm q, \pm r)$. Note

that $\{\mathbf{H}^{\mathrm{m}}_{\mathrm{xz}}(\mathbf{Q_i})\,\mathrm{e}^{\mathrm{i}\,\mathbf{Q_i}\cdot\mathbf{x}}\}$ form an orthonormal set, if all $\mathbf{H}^{\mathrm{m}}_{\mathrm{xz}}(\mathbf{Q_i})$ are normalized so as to have unit norm $|\mathbf{H}^{\mathrm{m}}_{\mathrm{xz}}(\mathbf{Q_i})| = 1$.

Two findings important for later arguments can be extracted from (10) and (11). First, resonant modes in the cube are equivalent to the linear combination of plane waves proportional to the Bloch modes satisfying the Bragg condition and propagating in the multiperiodic lattice, as previously analyzed (Note that the Bloch modes have wavenumber $\mathbf{k} = -1/2\mathbf{P_n} = \mathbf{P}_{-\mathbf{n}/2}$ under the Bragg condition, and that $\{\mathbf{P}_{\mathbf{n}/2}\} \supset \{\mathbf{Q_i}\}$). Therefore, one uses the band theory only for the multiperiodic lattice already in hand, in order to investigate the coupling between the Bloch and resonant modes, despite the fact that a PF is not a periodic structure but isolated. Second, since it can be seen that the Bloch mode satisfying the Bragg condition manifestly degenerates to the resonant mode specified by the same index as the Bloch, they could easily couple in PFs without particular restrictions, and localized modes in PF never exist unless such restriction exists. Fortunately, the existence of the restrictions is demonstrated in subsequent sections.

4.3. Mode Coupling between Both Modes

4.3.1. Perturbation Theory 1: Correction to Bloch Modes

According to the strategy stated in Section 3, the next aim is to seek conditions such that the Bloch and resonant modes never couple in PFs. If these could be found, it can be deduced that certain resonant modes might survive as localized modes in PFs. To carry out the search, a perturbative treatment is thought to be optimum. Therefore, we first derive a perturbation-approximated representation of the correlation amplitude between the two modes. To begin, we will take Maxwell's equation for PFs by replacing $L^N(\mathbf{x})$ in (7) with $M^N(\mathbf{x})$. Next, we rewrite (4) using $\nabla \times \{f(\mathbf{x})\nabla\times\} \equiv D\big(f(\mathbf{x})\big)$ and magnetic field $\mathbf{H}(\mathbf{x}) \equiv |\,\varphi\,\rangle\!\rangle$ which is a solution asymptotically closing to a Bloch mode, for easy notation. Then, in order to treat the correlation between the two modes as the influence of potential $M^N(\mathbf{x})$ upon the Bloch modes, if one regards $M^N(\mathbf{x}) - L^N(\mathbf{x})$ as a first-order infinitesimal quantity, Maxwell's equation for $M^N(\mathbf{x})$ can be described as

$$\{D(1) - \varepsilon_f^{-1} D(L^N)\}\,|\,\varphi\,\rangle\!\rangle - \varepsilon_f^{-1} D(V)\,|\,\varphi\,\rangle\!\rangle = W\,|\,\varphi\,\rangle\!\rangle\,. \qquad (12)$$

Here, $V \equiv M^N - L^N = L^N(C-1)$ (hereinafter, position $\mathbf{x}$ will be suppressed). After inserting $|\,\varphi\,\rangle\!\rangle$ and W which are perturbatively

expanded by Bloch modes $\{|\,\mathbf{n}\,\rangle\!\rangle\}$ defined in Section 4.1.1 and corresponding correction terms

$$|\,\varphi\,\rangle\!\rangle = |\,\mathbf{m}\,\rangle\!\rangle + \sum_{\mathbf{n}} c_{\mathbf{mn}}|\,\mathbf{n}\,\rangle\!\rangle + \dots \tag{13a}$$

$$W = W_{\mathbf{m}}^{(0)} + W_{\mathbf{m}}^{(1)} + \dots \tag{13b}$$

into (12), and simplifying using (14a); Maxwell's equation for the zeroth order Bloch modes $\{|\,\mathbf{n}\,\rangle\!\rangle\}$ in multiperiodic lattice $L^N(\mathbf{x})$, and (14b); the orthogonality relation for the modes,

$$\left\{D(1) - \varepsilon_f^{-1} D\left(L^N\right)\right\} |\,\mathbf{m}\,\rangle\!\rangle = W_{\mathbf{m}}^{(0)}|\,\mathbf{m}\,\rangle\!\rangle \tag{14a}$$

$$\langle\!\langle\,\mathbf{m}\,|\,\mathbf{n}\,\rangle\!\rangle = \delta_{\mathbf{mn}}, \tag{14b}$$

and then taking an inner product with the resonant mode $|\mathbf{i})$ (note that suffixes "m" and "xy" for the mode classification and parity, respectively, are also suppressed), and then picking up the first order infinitesimal quantities, finally the following correlation amplitude between the two modes is derived.

$$(\mathbf{i}|\,\varphi\,\rangle\!\rangle = (\mathbf{i}|\,\mathbf{m}\,\rangle\!\rangle + \varepsilon_f^{-1} \sum_{\mathbf{n}} \frac{\langle\!\langle\,\mathbf{n}|D(V)|\mathbf{m}\,\rangle\!\rangle}{W_{\mathbf{n}}^{(0)} - W_{\mathbf{m}}^{(0)}} (\mathbf{i}|\,\mathbf{n}\,\rangle\!\rangle \tag{15}$$

Hereinafter, we should focus on the situation where the Bragg condition for $L^N(\mathbf{x})$ is satisfied, because we must analyze the mode coupling between the Bloch and the resonant modes, and because the both modes indeed degenerate in this situation as stated below. In this situation, the following consequences result. First, if one chooses $|\,\mathbf{n}\,\rangle\!\rangle$ and $|\,\mathbf{m}\,\rangle\!\rangle$ having the same eigenvalue, the second term of the right-hand-side of (15) becomes dominant, and the first term is negligibly small, because $W_{\mathbf{n}}^{(0)} = W_{\mathbf{m}}^{(0)}$ is satisfied. This is the same argument involved in the conventional approximation imposed for deriving band gaps in Section 4.1.1. Second, as concluded in Section 4.2, resonant modes $\{|\mathbf{i})\}$ are approximately equal to the linear combination of degenerating Bloch modes $\{|\,\mathbf{i}\,\rangle\!\rangle\}$. Accordingly, one can replace $|\mathbf{i})$ in (15) with the associated $|\,\mathbf{i}\,\rangle\!\rangle$ (this point is quite significant for reducing subsequent perturbation calculations). Third, when calculating inner products between two Bloch modes $|\,\mathbf{n}_1\,\rangle\!\rangle$ and $|\,\mathbf{n}_2\,\rangle\!\rangle$, one can generically obtain the same results as those calculated from $|\,\mathbf{0}\,\rangle\!\rangle$ and $|\,\mathbf{n}_1 - \mathbf{n}_2\,\rangle\!\rangle$ because of the translational symmetry for lattices. Incorporating the above three facts into (15), the correlation amplitude can be written only for Bloch modes as follows.

$$(\mathbf{i}|\,\varphi\,\rangle\!\rangle \propto \varepsilon_f^{-1}\,\langle\!\langle\,\mathbf{n}|D(V)|\mathbf{0}\,\rangle\!\rangle\,\langle\!\langle\,\mathbf{i}|\mathbf{n}\,\rangle\!\rangle \tag{16}$$

It can be determined from this expression that resonant mode $|\mathbf{i})$ never couples in PFs to $|\,\varphi\,\rangle\!\rangle$ which is a Bloch mode receiving the first perturbation correction, as long as $\langle\!\langle\,\mathbf{n}|D(V)|\mathbf{0}\,\rangle\!\rangle = 0$ holds, even if field distributions of the resonant mode perfectly coincide with those of the Bloch mode, namely $\langle\!\langle\,\mathbf{i}|\mathbf{n}\,\rangle\!\rangle \neq 0$ ($\langle\!\langle\,\mathbf{i}|\mathbf{n}\,\rangle\!\rangle \neq 0$ means a mode coincidence $\mathbf{i} = \mathbf{n}$ because of (5b) expressing the orthogonality of Bloch modes). Therefore, if the mode $|\,\mathbf{i}\,\rangle\!\rangle$ satisfying $\langle\!\langle\,\mathbf{i}|D(V)|\mathbf{0}\,\rangle\!\rangle = 0$ could be concretely identified, it leads to the crucial finding that there exist resonant modes that never couple to Bloch modes and that remain localized modes in PFs, and hypothesis (2) is thereby illustrated.

We proceed to reveal the physical meaning of $\langle\!\langle\,\mathbf{i}|D(V)|\mathbf{0}\,\rangle\!\rangle = 0$ by concrete calculation. If one uses the expression of Bloch modes including magnetic polarization, namely $|\,\mathbf{m}\,\rangle\!\rangle \propto \mathbf{H}(\mathbf{m})\,\mathrm{e}^{\mathrm{i}(\mathbf{k}+\mathbf{P_m})\cdot\mathbf{x}}$, (14a) and (14b), and the following formulae concerning the convolution integral between any two sinc functions:

$$\begin{aligned}\int d^3q\ \operatorname{sinc}\frac{d}{2}(\mathbf{A}-\mathbf{q})\operatorname{sinc}\frac{d}{2}\mathbf{q} &= \left(\frac{2\pi}{d}\right)^3 \operatorname{sinc}\frac{d}{2}\mathbf{A},\\ \int d^3q\ \mathbf{q}\operatorname{sinc}\frac{d}{2}(\mathbf{A}-\mathbf{q})\operatorname{sinc}\frac{d}{2}\mathbf{q} &= \left(\frac{2\pi}{d}\right)^3 \frac{\mathbf{A}}{2}\operatorname{sinc}\frac{d}{2}\mathbf{A}\\ &= \mathbf{0}\quad (\text{if } \mathbf{A}\in\{\mathbf{P_n}\}),\end{aligned} \tag{17}$$

then the following result is obtained.

$$\langle\!\langle\,\mathbf{i}|D(V)|\mathbf{0}\,\rangle\!\rangle = -\frac{1}{4}\,|\mathbf{P_i}|^2\,\{\mathbf{H}^*(\mathbf{i})\cdot\mathbf{H}(\mathbf{0})\}\,L^N(\mathbf{i}) \tag{18}$$

From (18), an important consequence, that is, $\langle\!\langle\,\mathbf{i}|D(V)|\mathbf{0}\,\rangle\!\rangle \propto L^N(\mathbf{i})$, can be extracted, since generally $\mathbf{H}^*(\mathbf{i})\cdot\mathbf{H}(\mathbf{0}) \neq 0$. This claims that the resonant mode specified by index $\mathbf{i}$ must become a localized mode of PFs, if the Fourier coefficient $L^N(\mathbf{i})$ for the Bloch mode with the same index in the multiperiodic lattice of Stage-N equals zero.

One can still proceed to simplify (18) using the fact that perturbation calculations must be performed within the first-order approximation, and therefore one ought to eliminate higher infinitesimal quantities included in $L^N(\mathbf{i})$. As in Section 4.1.1, $L^{(1)}(\mathbf{0})$, $L^{(1)}(\mathbf{i})$, ($\mathbf{i} \neq \mathbf{0}$), and $L^{(1)}(\mathbf{j})$, ($\mathbf{i} \neq \mathbf{j}$) are infinitesimal quantities of the zeroth order, the first order, and orders greater than the second, respectively. Hence, leaving terms until the first order in $L^N(\mathbf{i})$ with using (9a), the following results are derived.

$$L^N(\mathbf{i}) \approx L^{(1)}(\mathbf{i})\Big\{L^{(1)}(\mathbf{0})\Big\}^{N-1} = L^{(1)}(\mathbf{i})\left(\frac{20}{27}\right)^{N-1} \tag{19}$$

Consequently, this means $\langle\langle\, \mathbf{i}|D(V)|\mathbf{0}\,\rangle\rangle \propto L^{(1)}(\mathbf{i})$. According to this outcome and the findings derived in Sections 4.1.2 and 4.2, $\langle\langle\, \mathbf{i}|D(V)|\mathbf{0}\,\rangle\rangle = 0$ holds for a Bloch mode specified by index vector $\mathbf{i} = (3l, m, n)$, ($l(\neq 0), m$ and n are integers) or permuted vectors of $\mathbf{i}$. As the Bloch mode is proportional to a resonant mode having a wavenumber $\mathbf{Q_i} = \mathbf{P}_{\mathbf{i}/2}$, it is deduced that the resonant mode never couples to Bloch modes then. Also, as investigated in Section 4.1.2, since band gaps assigned by any index vectors other than those with at least one component equal to multiples of 3^N for the multiperiodic lattice with Stage-N always appear, it follows that

A localized mode in PFs with Stage-N can be identified as a resonant mode in a paraelectric cube with the same side length and permittivity as those of the PF. In addition, the resonant mode with wavenumber $\mathbf{Q_i}$ *is specified only by index vector* $\mathbf{i} = (3l, m, n)/2$ *(* $l\,(\neq 0)$*,* m *and* n *are integers; however,* $3l$*,* m *and* n *unequal to multiples of* 3^N*) or permuted vectors of* $\mathbf{i}$*.*

is deduced, within the scope of the first perturbation approximation with evanescent magnetic fields exuding on surfaces of the cube are omitted. Consequently, the generating mechanism for localized modes in the PF hypothesized as (2) is now fully justified by the above calculations. Expressing this outcome simply, as resonant and Bloch modes cannot interact with each other under the above situation and they cannot mix together, then the former is isolated and emerges as a localized mode in band gaps generated by the multiperiodic lattice contained in the PF.

4.3.2. Perturbation Theory 2: Correction to Resonant Modes

The perturbation calculations performed below are concerned with the first-order corrections by $M^N - C$ to resonant modes $\{|\mathbf{i})^{\mathrm{m}}_{\mathrm{xz}}\}$ in contrast to the preceding subsection. We will investigate how resonant frequencies for the modes are modified. The calculation processes taken here are almost the same as the previous ones. Using the same notation as the previous subsection, and perturbation-approximately expanding a solution asymptotically closing to resonant mode $|\mathbf{i})^{\mathrm{m}}_{\mathrm{xz}}$ and an eigenvalue corresponding to the mode until the first order, the following expression of the first-order corrected eigenvalue can be derived from Maxwell's equiation for M^N.

$$W = \frac{|\omega_{\mathbf{i}}|^2}{c^2} - \varepsilon_f^{-1}(\mathbf{i}|\, D(C\{L^N - 1\})\,|\mathbf{i}) \tag{20}$$

Here the suffixes "m" (TE or TM) and "xy" (the parity with respect to x- and y-axes) are also suppressed as they were above.

Since it can be seen from (10) that modes with the same $|\mathbf{i}|$ have identical resonant frequencies despite the suffixes "m" and "xy" (namely, all of them degenerate), and since the perturbation $D(C\{L^N - 1\})$ possesses the same point symmetry as mode $|\mathbf{i}\rangle$ (i.e., introducing the perturbation cannot resolve the degeneracy), one can proceed with calculations for (20) using only any single term (which, however, must be normalized so as to have the unit norm) in the right-hand-side of (11), for example $\mathbf{e}\,\mathrm{e}^{\mathrm{i}\,\mathbf{Q_i}\cdot\mathbf{x}}$, ($|\mathbf{e}|^2 = 1$). Moreover, as $\mathbf{k}+\mathbf{P_i} = \mathbf{Q_i}$ holds under the Bragg condition, and the field distribution $\mathbf{e}\,\mathrm{e}^{\mathrm{i}\,\mathbf{Q_i}\cdot\mathbf{x}}$ equals $\mathbf{e}|\mathbf{i}\rangle$, we can perform subsequent calculations to set $|\mathbf{i}) = \mathbf{e}|\mathbf{i}\rangle$. Then, by applying (17) and $|\mathbf{e}|^2 = 1$ to $\langle\mathbf{i}|\,D(C\{L^N - 1\})\,|\mathbf{i}\rangle$ with arbitrary wavenumber $\mathbf{k}$, the following equation is obtained after some manipulation.

$$\langle\mathbf{i}|\,D(C\{L^N - 1\})\,|\mathbf{i}\rangle = \{L^N(\mathbf{0}) - 1\}\,(\mathbf{k} + \mathbf{P_i})^2 \tag{21}$$

Then, setting $\mathbf{k}$ so as to satisfy the Bragg condition and inserting (21) into (20), W can be reduced to the following simple expressions.

$$W = \left(1 - \varepsilon_f^{-1} L^N(\mathbf{0})\right)|\mathbf{Q_i}|^2 = \overline{\left(\frac{1}{\varepsilon_r(\mathbf{x})}\right)}|\mathbf{Q_i}|^2 = \frac{1}{\bar{\varepsilon}_r}|\mathbf{Q_i}|^2 \tag{22}$$

Here, the fact that the first term on the right-hand-side of (20) satisfies the dispersion relation $\varepsilon_r\,{\omega_\mathbf{i}}^2 = c^2|\mathbf{Q_i}|^2$, is used for the reduction. In addition, the translation of $L^N(\mathbf{0})$ into $\varepsilon_r(\mathbf{x})$ can be obtained from (6a) and (7).

If one writes a resonant frequency for the mode undergoing the first perturbation correction as $\omega_\mathbf{i}^{(1)}$, the dispersion relation $W = (\omega_\mathbf{i}^{(1)})^2/c^2$ ought to hold. Also, replacing $\omega_\mathbf{i}^{(1)}$ with the wavenumber in free space, k_0, satisfying the dispersion relation $\omega_\mathbf{i}^{(1)} = c\,k_0$, the following simple equation results as the resonance condition for the localized mode in the PF.

$$|\mathbf{Q_i}|^2 = \bar{\varepsilon}_r\,{k_0}^2 \tag{23}$$

If one focuses on a set of localized modes specified by $\mathbf{i} = (3l, 0, 0)/2$, ($3l \neq$(multiples of 3^N)), the following resonance conditions, including (1) as the fundamental resonance, are finally derived for a PF with Stage-N.

$$d = \frac{3}{2}\frac{\lambda_0}{\sqrt{\bar{\varepsilon}_r}}\,|l|, \quad (l \neq 3^{N-1}) \tag{24}$$

At last, the hypothesis (2) is affirmatively and concretely demonstrated. Also, it was disclosed that localized modes in the PF originate from the resonant modes in a cubic structure contained in the PF, which do not couple with Bloch modes propagating in a multiperiodic lattice also contained in the PF, and which appear in band gaps of the lattice.

5. CONSIDERATIONS

As demonstrated in previous sections, the generic resonance condition, including the experimental result (1), was correctly derived in the scope of the first perturbation theory by the introduction of a novel fractal construction method regarding an MS as a composite structure of a multiperiodic lattice and a paraelectric cube. This demonstrates hypothesis (2) concerning the generation mechanism of localized modes in PFs. By admitting this finding, other strange properties of PFs already reported (i.e., that no localized mode appears in PFs if the Stage-number becomes less than or equal to one [2], and the relationship between the arrangement of PFs so as to construct a two-dimensional lattice and the generation of a localized mode [6]), can be straightforwardly interpreted as follows. The former can be explained by a localized mode specified by $\mathbf{i} = (3l, 0, 0)/2$, ($3l \neq$ (multiples of 3^N)) appearing in a "closed" band gap formed by Bloch modes if one sets the Stage-number N to less than or equal to one, and never being observed. The latter can be explained by the mode coupling between localized modes originally generated by an isolated PF and new Bloch modes determined by the arrangement of PFs. Namely, if one designs the periodicity of the lattice so that the degeneracy between the localized and the Bloch modes is resolved, the former must be observed in scattering spectra, because two conditions (coupling between both modes does not occur, and the former appears in band gaps defined by the latter) are fulfilled.

Fractal structures different from MSes but constructed by way of the same geometrical manipulations as shown in this report can also be easily investigated by tracing the discussions developed above for mode analysis. For example, resonance conditions for localized modes in an MS with a self-similarity homothetic ratio other than 1/3 or a potential other than the hexapod will be easily considered.

Furthermore, we can develop a conjecture about the experimental result in which a PF shows a resonant Q higher than the one defined by the inverse of dielectric loss possessed by the composing medium. Specifically, this could be attributed to the reduction of effective dielectric loss expected considering that electromagnetic energy might

localize mainly at the outside of the constituent paraelectric [2, 3, 10], and to the decrease of radiation losses due to the difficulty in propagating evanescent fields because PFs are surrounded by band gaps of the multiperiodic lattice as shown in this report (note that the latter can be compared to a point-defect resonator embedded in a photonic crystal [14]). From an engineering viewpoint, this property of PFs is attractive for realizing a physically small high-Q resonator; however, some discrepancies of the Q between experimental and numerical studies were observed [8]. The treatment taken in this report is still insufficient to tackle this issue, and further theoretical development should be indispensable.

Few experimental results still cannot be understood only by the discussion developed in this report, for example, experimental resonance conditions for higher-order localized modes [5]. In order to improve the accuracy of analyses, if one relaxes one of above-applied approximations, that the exudation of evanescent fields existing on the outsides of the paraelectric cube are negligible small, then the degeneracy of localized modes is resolved, and more modes ought to be generated than the experimental result. This conflict might be solved theoretically if higher-order perturbation corrections or the non-perturbative treatment are taken into account. In addition, localized modes in a metallic PF [7] are also outside the scope of this analysis (one must be able to treat this problem by using spectral domain approach [15], applied to waveguides with Šerpinskij Carpet-like sections [16]. Numerical analyses of metallic MSes by the finite-difference time-domain (FDTD) method are reported in Reference [7]). Thus we hope that theoretical developments for these lines will progress further.

6. CONCLUSION

The origin of strange electromagnetic resonant phenomena, known as localized modes and generated in a photonic fractal that is an isotropic paraelectric Menger sponge (MS), was theoretically revealed. Generic resonance conditions embracing experimental results for the fundamental mode were also derived. These findings could be extracted by treating the MS not as a fractal structure resulting from the conventional construction method for a self-similar configuration, but as a dielectric cube embedded in a multiperiodic lattice represented as the product of a number of simple lattices with different lattice constants, and by applying the first perturbation theory for analyzing the mode coupling among two set of modes supported by the two constituent structures in the MS. From the results, it was deduced that

the localized modes can be identified with resonant modes, originally generated in the dielectric cube, that appear in band gaps generated by Bloch modes for the lattices and never couple to Bloch modes. Other experimental results could also be qualitatively understood from the revealed findings.

REFERENCES

1. Feder, J., *Fractals*, Plenum Press, New York, 1988.
2. Takeda, M. W., S. Kirihara, Y. Miyamoto, K. Sakoda, and K. Honda, "Localization of electromagnetic waves in three-dimensional fractal cavities," *Phys. Rev. Lett.*, Vol. 92, No. 093902, 2004.
3. Kirihara, S., Y. Miyamoto, M. W. Takeda, K. Honda, and K. Sakoda, "Strong localization of electromagnetic wave in ceramic/epoxy photonic fractals with Menger-sponge structure," *Proc. on Ceramic Engineering and Science*, Vol. 26, No. 3, 367–372, 2005.
4. Semouchkina, E., Y. Miyamoto, S. Kirihara, G. Semouchkin, and M. Lanagan, "Analysis of electromagnetic response of 3-D dielectric fractals of Menger sponge type," *IEEE Trans. Microw. Theory Tech.*, Vol. 55, No. 6, 1305–1313, 2007.
5. Miyamoto, Y., H. Kanaoka, and S. Kirihara, "Terahertz wave localization at a three-dimensional ceramic fractal cavity in photonic crystals," *J. Appl. Phys.*, Vol. 103, No. 10, 103106.1–103106.5, 2008.
6. Mori, A., S. Kirihara, Y. Miyamoto, M. W. Takeda, K. Honda, and K. Sakoda, "Integration of ceramic/epoxy photonic fractals with localization of electromagnetic waves," *Proc. on Ceramic Engineering and Science*, Vol. 26, No. 3, 361–366, 2005.
7. Sakoda, K., "Scaling property and symmetry-dependent escape time of the localized electromagnetic modes in the metallic Menger sponge fractal," *Laser Physics*, Vol. 18, No. 12, 1378–1385, 2008.
8. Sakoda, K., "Electromagnetic eigenmodes of a three-dimensional photonic fractal," *Phys. Rev. B*, Vol. 72, No. 18, 184201, 2005.
9. Sangawa, U., "Non-resonant electromagnetic scattering properties of Menger's sponge composed of isotropic paraelectric material," *IEICE Trans. Electron.*, Vol. E90-C, No. 2, 484–491, 2007.
10. Sangawa, U., "Resonance analysis of multilayered filters with triadic Cantor-type one-dimensional quasi-fractal structures," *IEICE Trans. Electron.*, Vol. E88-C, No. 10, 1981–1991, 2005.

11. Itoh, T. and C. Chang, "Resonant characteristics of dielectric resonators for millimeter-wave integrated circuits," *Proc. IEEE Microw. Theory Tech. Soc. Int. Symp.*, Vol. 78, No. 1, 121–123, 1978.
12. Marcatili, E. A. J., "Dielectric rectangular waveguide and directional coupler for integrated optics," *Bell Syst. Tech. J.*, Vol. 48, 2071–2102, 1969.
13. Zhang, K. and D. Li, *Electromagnetic Theory for Microwaves and Optoelectronics*, 2nd editon, 348–352, Springer, New York, 2007.
14. Noda, S., A. Chutinan, and M. Imada, "Trapping and emission of photons by a single defect in a photonic bandgap structure," *Nature*, Vol. 407, 608–610, 2000.
15. Itoh, T., "Spectral domain immitance approach for dispersion characteristics of generalized printed transmission lines," *IEEE Trans. Microw. Theory Tech.*, Vol. 28, No. 7, 733–736, 1980.
16. Arrighetti, W. and G. Gerosa, "Spectral analysis of Šerpinskij carpet-like prefractal waveguides and resonators," *IEEE Microw. Wireless Compon. Lett.*, Vol. 15, No. 1, 30–32, 2005.